Turbulence Characteristics of Flow in a Two Dimensional Contraction

M. M. Rahman [1] and T. Siikonen [2]

Helsinki University of Technology, Department of Mechanical Engineering,
Laboratory of Applied Thermodynamics, Sähkömiehentie 4, FIN-02015 HUT
Finland

Abstract — The relaminarization of a fully turbulent flat plate boundary layer subjected to a favorable pressure gradient inside a two-dimensional contraction has been carried out numerically. Two low-Reynolds number isotropic k-$\tilde{\epsilon}$ models are employed in the simulation. The simulated fluid flow and turbulence characteristics are compared with the experiment, demonstrating that the models have good agreement with the data as the flow approaches the laminar state.

Key Words: Contraction, turbulence, relaminarization, boundary layer.

Introduction

Plane contraction is associated with the hydraulic head box utilized in the paper manufacturing machine. It is characterized by the presence of a two-dimensional contracting part, mounted at the end of a step diffuser. In this device the flow is contracted in one direction and hence pragmatically called as the "two-dimensional contraction". The paper manufacturer presumably pays attention to the determination of turbulence characteristics of the flow through this contraction. The reasoning is that the mechanical properties of the paper may considerably depend on the turbulence phenomena.

Experiments show that the acceleration through the contraction suppresses the relative turbulence intensities, which have almost no effect on the mean velocity distributions in the contraction. The streamwise component of the Reynolds stresses decays on passing through the contraction, whereas the transverse components grow equally. A reduction in the contraction angle brings about an increased decay rate of the turbulence. Another phenomenon is the relaminarization of turbulent boundary layer subjected to a favorable pressure gradient due to acceleration in the contraction. Herein the turbulent bursts near the wall disappear, the law of the wall breaks down and the turbulent intensity shows a tendency to decay. In principle, the shear stress distribution in the wall region rather than the Reynolds number is the most important factor for the occurrence of boundary layer relaminarization. The ultimate penalty due to the relaminarization is a significant reduction in the friction/heat transfer coefficient.

Unambiguously, the flow structure is inherently connected with the industrial application. Therefore, it can be considered as a test case for the turbulence modeling. However, inadequate attempt has been made in computing the flow contraction due to the complexity in flow struc-

[1] Research Scientist, Department of Mechanical Engineering
[2] Professor, Department of Mechanical Engineering

ture and unavailability of suitable turbulent models. Unfortunately, the configuration lacks in sufficient experimental data.

In this study the flow inside a two-dimensional converging channel is simulated at a Reynolds number $Re \approx 5.2 \times 10^4$. Particular attention is paid to the relaminarization in the boundary layer of a flat plate, positioned at the centerline of the contraction. Two low-Reynolds number linear k-$\tilde{\epsilon}$ models, namely the original Chien (OCH) model [2] and the modified Chien (MCH) model [3] participate in the simulation. Computed velocity profiles and turbulent intensities are compared with the experimental data of Ref. [4].

Turbulence Modeling

The two-dimensional Reynolds-averaged Navier-Stokes ($RANS$) equations, including the equations for the kinetic energy k and dissipation $\tilde{\epsilon}$, can be written in the following form:

$$\frac{\partial U}{\partial t} + \frac{\partial (F - F_v)}{\partial x} + \frac{\partial (G - G_v)}{\partial y} = Q \tag{1}$$

where $U = (\rho, \rho u, \rho v, E, \rho k, \rho\tilde{\epsilon})^T$. The inviscid fluxes are

$$F = \begin{pmatrix} \rho u \\ \rho u^2 + p + \frac{2}{3}\rho k \\ \rho uv \\ u(E + p + \frac{2}{3}\rho k) \\ \rho uk \\ \rho u\tilde{\epsilon} \end{pmatrix}, \qquad G = \begin{pmatrix} \rho v \\ \rho vu \\ \rho v^2 + p + \frac{2}{3}\rho k \\ v(E + p + \frac{2}{3}\rho k) \\ \rho vk \\ \rho v\tilde{\epsilon} \end{pmatrix} \tag{2}$$

Here ρ is the density and p is the pressure. The total energy is defined as

$$E = \rho e + \frac{\rho \vec{V} \cdot \vec{V}}{2} + \rho k \tag{3}$$

where e is the specific internal energy and $\vec{V} = u\vec{i} + v\vec{j}$ is the velocity . The viscous fluxes are

$$F_v = \begin{pmatrix} 0 \\ \tau_{xx} + \frac{2}{3}\rho k \\ \tau_{xy} \\ u\tau_{xx} + v\tau_{xy} - q_x \\ \mu_k(\partial k/\partial x) \\ \mu_\epsilon(\partial\tilde{\epsilon}/\partial x) \end{pmatrix}, \qquad G_v = \begin{pmatrix} 0 \\ \tau_{xy} \\ \tau_{yy} + \frac{2}{3}\rho k \\ u\tau_{xy} + v\tau_{yy} - q_y \\ \mu_k(\partial k/\partial y) \\ \mu_\epsilon(\partial\tilde{\epsilon}/\partial y) \end{pmatrix} \tag{4}$$

and the viscous stress tensor can be given as

$$\tau_{ij} = \mu \left(\frac{\partial u_j}{\partial x_i} + \frac{\partial u_i}{\partial x_j} - \frac{2}{3}(\nabla \cdot \vec{V})\delta_{ij} \right) - \rho\overline{u_i u_j} \tag{5}$$

where μ is the laminar viscosity and $\rho\overline{u_i u_j}$ are the Reynolds stresses modeled using Boussinesq approximation. The heat flux is calculated from

$$\vec{q} = -(\lambda + \lambda_T)\nabla T = -\left(\mu \frac{c_p}{Pr} + \mu_T \frac{c_p}{Pr_T} \right) \nabla T \tag{6}$$

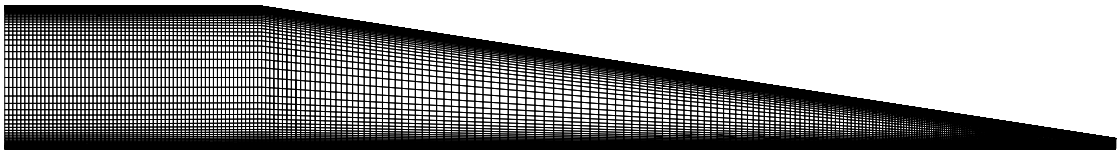

Figure 1: Computational grid for contracting channel.

where μ_T is the coefficient of turbulent viscosity, λ and λ_T are the laminar and turbulent thermal conductivity coefficients, Pr and Pr_T represent the laminar and turbulent Prandtl numbers, and T and c_p imply the temperature and specific heat at constant pressure, respectively. Clearly, the turbulent part of the total heat-flux is estimated using Boussinesq approximation. The diffusion of turbulence is modeled as

$$\mu_k \nabla k = (\mu + \frac{\mu_T}{\sigma_k})\nabla k, \quad \mu_\epsilon \nabla \tilde{\epsilon} = (\mu + \frac{\mu_T}{\sigma_\epsilon})\nabla \tilde{\epsilon} \tag{7}$$

where σ_k and σ_ϵ are the appropriate empirical constants. The source term Q for the k and $\tilde{\epsilon}$ equations can be written as

$$Q = \begin{pmatrix} \rho P - \rho\epsilon + E_k \\ \dfrac{C_{\epsilon 1}\rho P - C_{\epsilon 2} f_2 \rho\tilde{\epsilon} - f_3 \rho D}{T_t} + E_\epsilon \end{pmatrix} \tag{8}$$

where $\epsilon = \tilde{\epsilon} + D$ and the turbulent production term $P = -\overline{u_i u_j}(\partial u_i / \partial x_j)$. The eddy viscosity and other variables are evaluated as

$$\begin{array}{rclrcl} \mu_T & = & C_\mu f_\mu \rho k T_t, & T_t & = & max\left(k/\tilde{\epsilon}, \sqrt{2\nu/\epsilon}\right) \\ D & = & 2\nu k / y_n^2, & y^+ & = & u_\tau y/\nu \\ R_y & = & \sqrt{k} y_n / \nu, & R_T & = & k^2/\nu\tilde{\epsilon} \end{array} \tag{9}$$

where u_τ is the friction velocity, y_n is the normal distance from the wall and ν represents the kinematic viscosity. The turbulence time scale T_t prevents the singularity at $y_n = 0$ in the dissipation equation.

The MCH model defines the near-wall damping function f_μ as a function of R_λ

$$\begin{array}{rcl} f_\mu & = & 1 - exp(-0.01 R_\lambda - 0.0068 R_\lambda^3) \\ R_\lambda & = & y_n / \sqrt{\nu\, T_t} \end{array} \tag{10}$$

where $\sqrt{\nu\, T_t}$ is the Taylor microscale. The quantities E_k and E_ϵ in Eq. (8) are known as cross-diffusion terms evaluated as [Rahman and Siikonen, 2000]

$$\begin{array}{rcl} E_k & = & C_k \mu_T\, min\left[\dfrac{\partial(k/\epsilon)}{\partial x_j}\dfrac{\partial\tilde{\epsilon}}{\partial x_j}, 0\right] \\ E_\epsilon & = & C_\epsilon \dfrac{\mu_T}{T_t^2}\left[\dfrac{\partial(k/\epsilon)}{\partial x_j}\dfrac{\partial k}{\partial x_j}\right] \end{array} \tag{11}$$

where the constants $C_k = 0.5$ and $C_\epsilon = -2C_k$. Table 1 summarizes functions and constants for different turbulence models.

Table 1: Functions and constants.

Model	D	$\tilde{\epsilon}_w$-B.C.	$C_{\epsilon 1}$	$C_{\epsilon 2}$	Pr_T	σ_k	σ_ϵ	C_μ
OCH	$2\nu\frac{k}{y_n^2}$	$\frac{\partial\tilde{\epsilon}}{\partial y_n}=0$	1.44	1.92	0.9	1.0	1.3	0.09
MCH	$2\nu\frac{k}{y_n^2}$	$\frac{\partial\tilde{\epsilon}}{\partial y_n}=0$	1.44	1.92	0.9	1.0	1.3	0.09

Model	f_μ	f_2	f_3	E_k	E_ϵ
OCH	$1.0-e^{-0.0115y^+}$	$1.0-0.22e^{-(R_T/6)^2}$	$e^{-0.5y^+}$	0.0	0.0
MCH	$Eq.(10)$	1.0	$e^{-(R_y/80)^2}$	$Eq.(11)$	$Eq.(11)$

Solution Method

A cell-centered finite-volume scheme together with an artificial compressibility approach is employed to solve the flow equations [5]. In the artificial compressibility method, the artificial compressibility is principally added to the derivative of density with respect to the pressure, influencing not only the continuity equation but also the other equations. The energy equation is not decoupled from the system of equations, facilitating a uniform treatment for both the primitive and conservative variables. A fully upwinded second-order spatial differencing is applied to approximate the convective terms. Roe's damping term [6] is used to calculate the flux on the cell face. A diagonally dominant alternating direction implicit (DDADI) time integration method [7] is applied for the iterative solution of the discretized equations. A multigrid method is utilized for the acceleration of convergence [8]. The basic implementation of the artificial compressibility method and associated features can be obtained [5, 9].

Results and Discussion

The reference velocity is $U_{ref} = 3.0m/s$ with an upstream turbulence intensity $Tu = 4.5\%$, defined as $Tu = \sqrt{\frac{2}{3}k}/U_{ref}$. The contraction inlet profiles for all dependent variables are generated by solving the models, invoking fully developed flow with $Re = U_{ref}L_{ref}/\nu \approx 5.2 \times 10^4$, where L_{ref} is the reference length at the contraction inlet. The contraction ratio $C = U_{out}/U_{ref}$ with a half angle of 9.16 become approximately 13. A 288×96 nonuniform grid having heavily clustered near the solid wall is used for the computations. The representative structured grid is displayed in Fig. 1. Two low-Reynolds number linear k-$\tilde{\epsilon}$ models, namely the OCH [2] and MCH [3] models are used in the simulations. Computed velocity profiles and turbulent intensities are compared with the experimental data [4]. All quantities shown below are normalized by the local maximum velocity corresponding to the position concerned.

Figure exhibits the mean velocity profiles at six representative positions. As is observed, the velocity defect in the outer region decreases in the presence of favorable pressure gradients. In addition, the boundary layer thickness continues to decrease as the flow develops downstream. The thickness of the last profile is approximately $1/20$ of that of the initial profile, indicating that the boundary layer approaches a laminar state.

Figure deals with the turbulence intensities at different downstream stations. It is evident upon investigation that predictions of the models are somewhat on a lower level than the data show at some positions. The agreement is better in the laminar region rather than in the turbulent region.

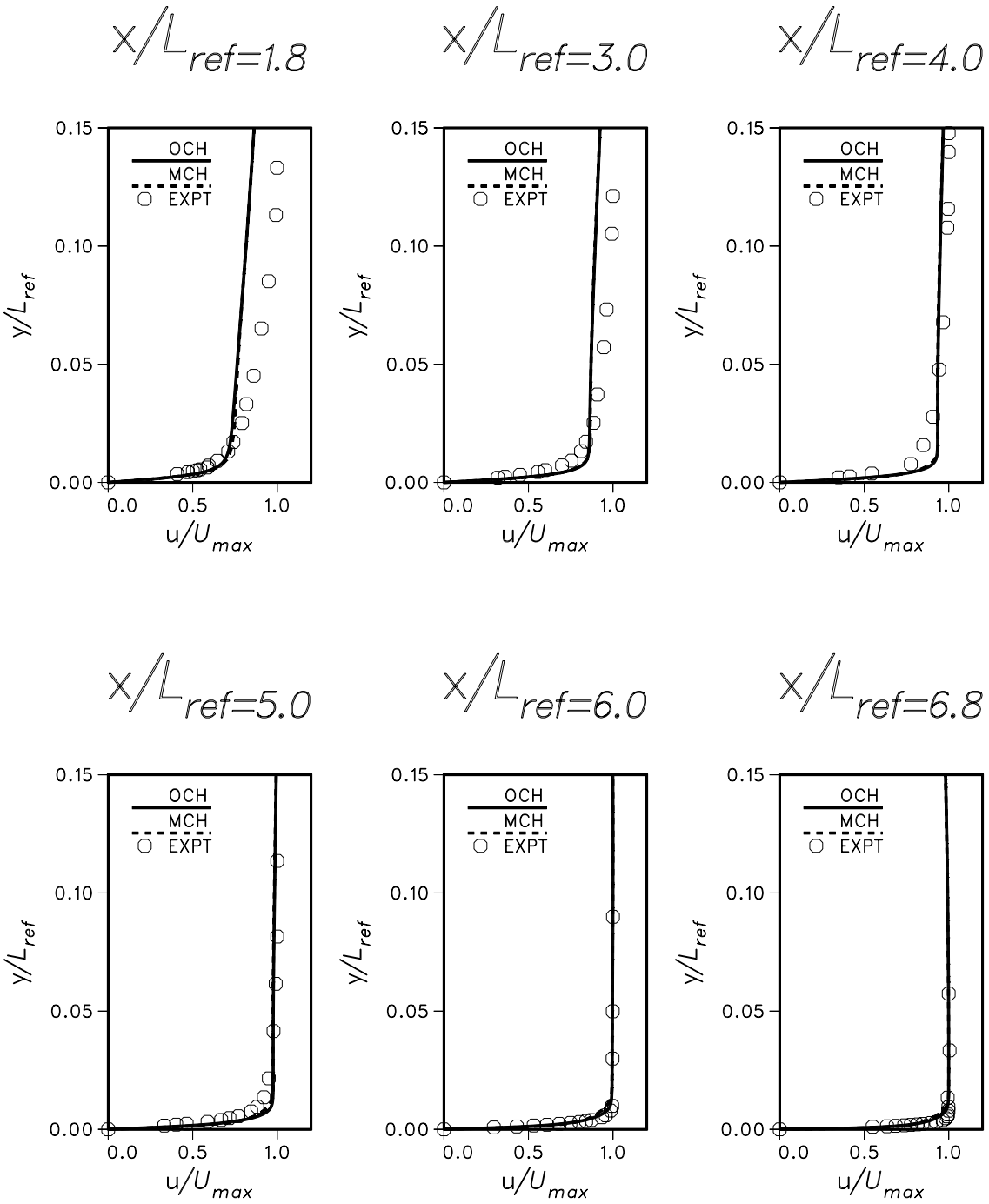

Figure 2: Velocity profiles at selected locations.

Conclusions

The characteristic of a initially turbulent boundary layer inside a two-dimensional contraction is numerically studied. The boundary layer thickness decreases with increasing distance from the contraction inlet and reaches about $1/20$ of that of the initial profile at the laminar region. Comprehensive comparisons conclude that the turbulent models maintain good correspondence with the experiments as the flow approaches the laminar state.

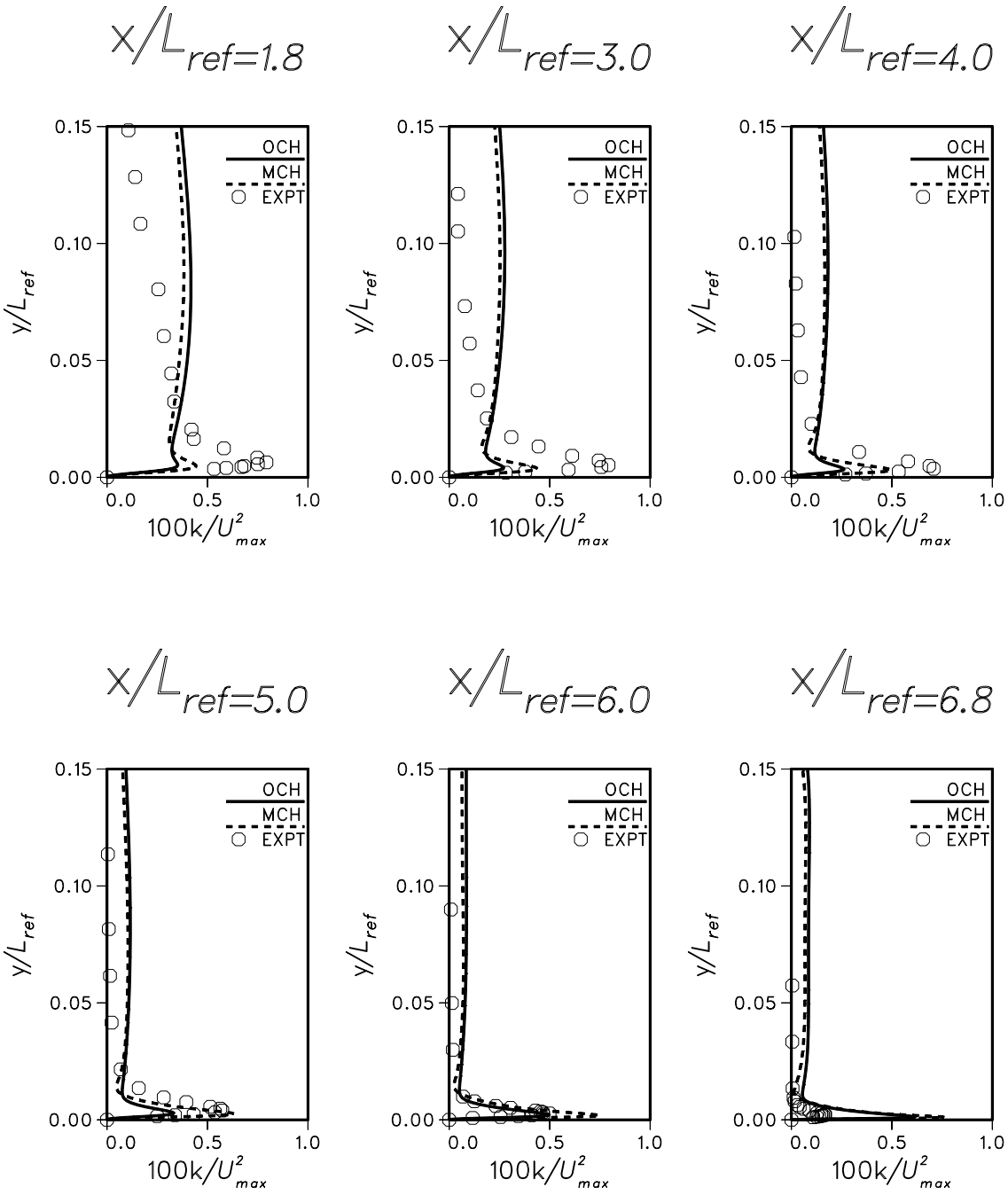

Figure 3: Kinetic energy profiles at selected locations.

REFERENCES

1. B. K. Yoon and M. K. Chung, ”Computation of Compression Ramp Flow with a Cross-Diffusion Modified k-ϵ Model”, *AIAA Journal*, Vol. 33, No. 8, 1995, pp. 1518-1521.
2. K-Y. Chien, ”Predictions of Channel and Boundary Layer Flows with a Low-Reynolds Number Turbulence Model”, *AIAA Journal*, Vol. 20, No. 1, 1982, pp. 33-38.
3. M.M. Rahman and T. Siikonen, ”Improved Low-Reynolds Number k-$\tilde{\epsilon}$ Model”, *AIAA J.*, 38, No. 7, 2000, pp. 1298-1300.
4. M. Parsheh, ”Flow in Contractions with Application to Headboxes”, *A Doctoral*

Thesis,2001, Royal Institute of Technology, Department of Mechanics, Faxenlaboratoriet, SE-100 44 Stockholm, Sweden.

5. M.M. Rahman, P. Rautaheimo and T. Siikonen, "Numerical Study of Turbulent Heat Transfer from a Confined Impinging Jet Using a Pseudo-Compressibility Method", *2nd International Symposium on Turbulence, Heat and Mass Transfer*, Delft Univ. Press, Delft, The Netherlands, 1997, pp. 511-520.
6. P.L. Roe, "Approximate Riemann Solvers, Parameter Vectors, and Difference Schemes", *J. Comput. Physics*, 43, 1981, pp. 357-372.
7. C. Lombard, J. Bardina, E. Venkatapathy and J. Oliger, "Multi-Dimensional Formulation of CSCM-an Upwind Flux Difference Eigenvector Split Method for the Compressible Navier-Stokes Equations", *6th AIAA Computational Fluid Dynamics Conference , AIAA Paper 83-1895-CP*, 1983, pp. 649-664.
8. A. Jameson and S. Yoon, "Multigrid Solution of the Euler Equations Using Implicit Schemes", *AIAA J.*, 24, 1986, pp. 1737-1743.
9. T. Siikonen, "An Application of Roe's Flux-Difference Splitting for $k-\epsilon$ Turbulence Model", *Int. J. Numer. Meth. Fluids*, 21, 1995, pp. 1017-1039.